

Steady-State Far-Infrared Coherent Synchrotron Radiation detected at BESSY II

M. Abo-Bakr, J. Feikes, K. Holldack, and G. Wüstefeld
BESSY mbH, Albert-Einstein-Straße 15, 12489 Berlin, Germany

H.-W. Hübers

DLR, Rutherford Strasse 2, 12489 Berlin, Germany

(Received 29 October 2001; revised manuscript received 8 April 2002; published 4 June 2002)

At BESSY II it is demonstrated that far-infrared coherent synchrotron radiation (CSR) can be generated by a controlled, steady-state process at storage rings. As an indication for coherent emission, the radiated power grows with the square of the beam current. The spectrum was analyzed by an interferometer in the 1-mm to 0.3-mm wavelength range. The CSR was enhanced more than 3000 times above background; the incoherent radiation remained below the background level. Steady-state and bursting CSR were discriminated by time resolved analysis from μ seconds to seconds.

DOI: 10.1103/PhysRevLett.88.254801

PACS numbers: 41.60.Ap, 29.20.-c

Coherent synchrotron radiation is a promising source of high intensity far-infrared radiation. The generation of CSR is well established in LINAC based sources [1]; in electron storage rings it is more difficult to achieve. CSR can be generated if the emitted electromagnetic waves superimpose at equal phase. For a given wavelength λ , the emitted radiative power P can be derived from the “incoherent” power P_λ emitted by a single particle

$$P = NP_\lambda(1 + Nf_\lambda),$$

where N is the number of electrons in the considered bunch volume and f_λ is a form factor, derived from the Fourier transform of the longitudinal electron bunch density [2]. In the case of a Gaussian density distribution of rms bunch length σ the form factor is simply given by $f_\lambda = \exp[-(2\pi\sigma/\lambda)^2]$. This relation states that short bunches and long wavelengths support CSR emission. The enhancement of the coherent compared to the incoherent power increases with the number of involved electrons, in our experiments typically 10^8 to 10^{10} . In the case where the bunch form factor f_λ is small, the huge number of involved electrons could still result in a large radiation enhancement, given by the product Nf_λ .

The vacuum chamber can cause long waves to become evanescent if the conducting surface is too close to the beam [2]. This sets an upper limit for the length of propagating waves, described by a cutoff wavelength. For the BESSY II [3] dipole chambers we calculate this cutoff to be ≈ 4 mm. This limits possible CSR emission from bunches of our regular machine optics, because the rms bunch length of > 5 mm is too long. Applying the Gaussian form factor a bunch length shorter than ≈ 2 mm seems necessary. Any deviation from a Gaussian bunch shape enhances the form factor and may lead to CSR detection of even longer bunches.

At some few storage rings CSR was observed [4] but always as a bursting emission process accompanied by longitudinal beam instabilities—a drawback for practical usage of CSR by synchrotron light users.

A way to manipulate bunch length (and shape) in storage rings directly is to tune the optics into a dedicated “low alpha mode,” where the “momentum compaction factor” α is controlled by the transverse beam optics [5]. Reducing α for a given electron momentum distribution $\Delta p/p$ leads to shorter bunches, formally related by $\sigma = |\alpha|R(\Delta p/p)f_{\text{rev}}/f_s$, where R is the average ring radius, f_{rev} the revolution frequency of the circulating electrons, and f_s the α -dependent longitudinal synchrotron oscillation frequency. Because beam current dependent effects lengthen the bunch, this σ is valid only in the limit of vanishing bunch current.

The “zero current” bunch length can be expressed as $\sigma = \sigma_0 f_s / f_{s0} = \sigma_0 \sqrt{|\alpha/\alpha_0|}$ at a fixed radio-frequency (rf) voltage. Because of this relation the bunch length is proportional to f_s . Different f_s values are determined from measured stripline signals. Typical values for the BESSY II user optics are $f_{\text{rev}} = 1.25$ MHz, $f_{s0} = 7.5$ kHz, $\alpha_0 = +7.3 \times 10^{-4}$, $\Delta p/p = 0.001$, and $\sigma_0 = 5$ mm. A low alpha optics was set up for the BESSY II storage ring, variable within $1 \times 10^{-6} < |\alpha| < \alpha_0$. The BESSY II double bend achromat optics is very flexible and well suited for this kind of optics, 4 families of sextupoles are available for controlling higher order terms of α and for chromatic and harmonic optics corrections. At a machine setting of $f_s = 2.3$ kHz ($\alpha = +7 \times 10^{-5}$) and a single bunch current of 0.25 mA the bunch length was found by a streak camera record to be $\sigma \approx 2$ mm [6].

In the presented experiments we mostly used moderate values $f_s > 1$ kHz ($|\alpha| > 1.5 \times 10^{-5}$) and 15 mA average beam current, resulting in a stable machine and a beam lifetime of some hours. In this mode the beam was stored as a multibunch filling in 100 consecutive bunches. The steady-state CSR was detected only in the low alpha mode tuned to values of $f_s < 3.5$ kHz.

In a second optics mode, the single bunch mode with values of f_{s0} and α_0 of the regular user optics, one bucket out of 400 empty buckets of the 500 MHz rf was filled with around 15 mA average beam current, corresponding

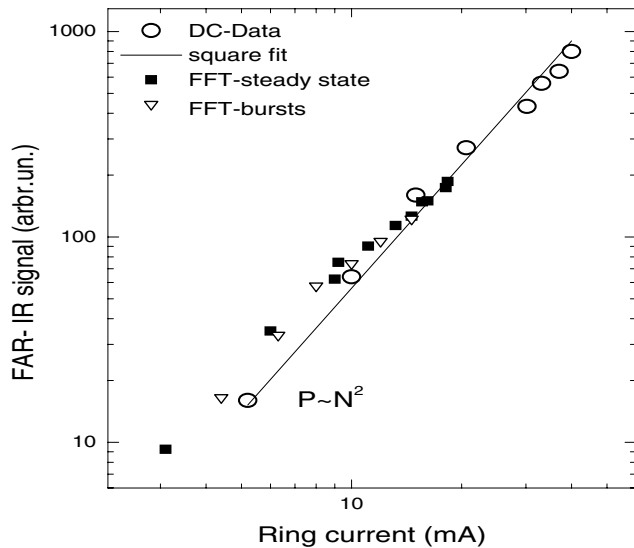


FIG. 1. Square dependency of the FIR signal amplitudes P as a function of the average beam current for the steady state and bursting case, (DC-Data are from [8]). The 3 data sets were normalized to equal signal strength at $I = 11$ mA.

to $N = 7.5 \times 10^{10}$ electrons per bunch. Bursting CSR was detected only in this mode.

For detecting the far-infrared (FIR) radiation an InSb hot electron bolometer [7] of about 5 mm^2 area was used. It has the highest responsivity of about 200 V/W in the wavelength range between 2 and 0.5 mm . The detector was placed 12 m away from the source point. The FIR dipole radiation was reflected by a plane mirror of 25 mrad^2 acceptance from the dipole fan to the floor above the ring, before being focused onto the detector by a mirror of short focal length. The detector entrance was shielded from visible light by a black polyethylene foil, while the vacuum ultraviolet and x-ray part cannot pass the mirror and the quartz vacuum chamber window.

To verify that the detected radiation is coherent, the signal strength as a function of the beam current was recorded at two different beam ports. In the previous one [8] (steady-state CSR), the IR radiation was guided from the source to the detector inside the vacuum and the signal strength was recorded by a dc voltage signal of the detector. In the present setup (steady-state and bursting CSR) the IR beam passed about 3 m of air before entering the detector. The IR signal is modulated with the beam revolution frequency and this modulation was enhanced by filling the ring only partly. This strongly modulated signal was recorded by a spectrum analyzer and shows an improved background-to-noise ratio compared to the previous method. Both approaches show roughly the I^2 dependency of the signal (see Fig. 1) in contrast to a linear relationship expected for the incoherent case.

Time and frequency resolved measurements are crucial to distinguish between bursting and steady-state mode. The time resolution of the detector as depicted in Fig. 2a shows FIR signals of the single bunch filling, with an empty time gap of 800 ns. The detector is biased in such a

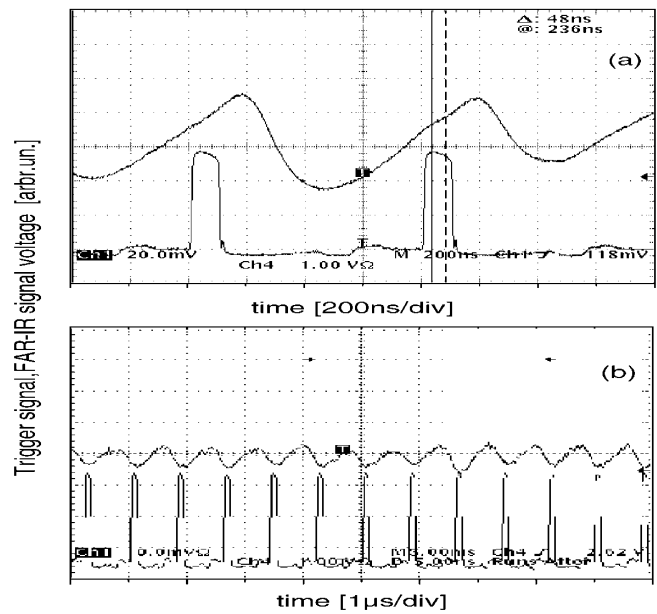


FIG. 2. Time resolved, sinelike FIR and needlelike, bunch revolution trigger signals for (a) bursting $I = 15$ mA, and (b) steady state mode, $I = 15$ mA, $f_s = 1.1 \text{ kHz}$ ($\alpha = -1.5 \times 10^{-5}$).

way that the signals show a negative deflection. Rise and fall time of the signal are 250 and 550 ns, respectively. The signal from the multibunch filling, 100 adjacent buckets filled, the subsequent 300 buckets empty, is shown in Fig. 2b. The empty time gap of 600 ns is still well resolved. In Fig. 3a FIR signals from the single bunch optics were accumulated for 500 ms by operating a scope in a persistent mode. The FIR signals were superimposed with the same phase as defined by the beam revolution trigger.

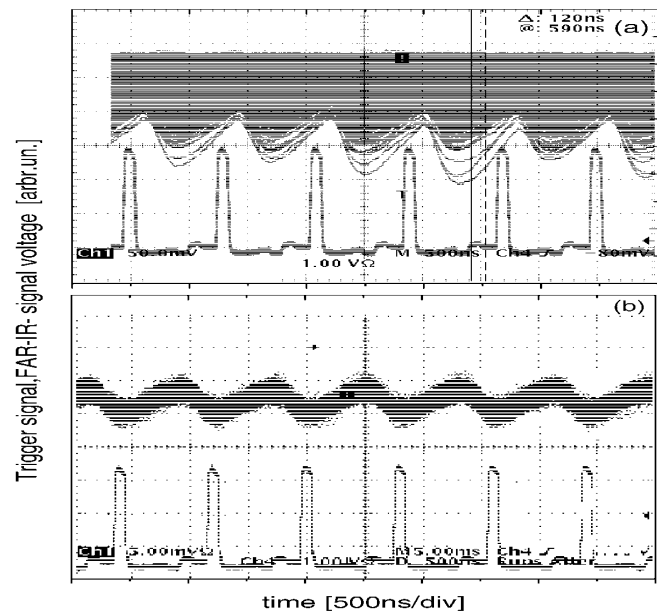


FIG. 3. FIR signals recorded in the persistent scope mode for (a) bursting, $I = 13.6$ mA and (b) steady state, $I = 15$ mA, $f_s = 1.1 \text{ kHz}$ ($\alpha = -1.5 \times 10^{-5}$) radiation.

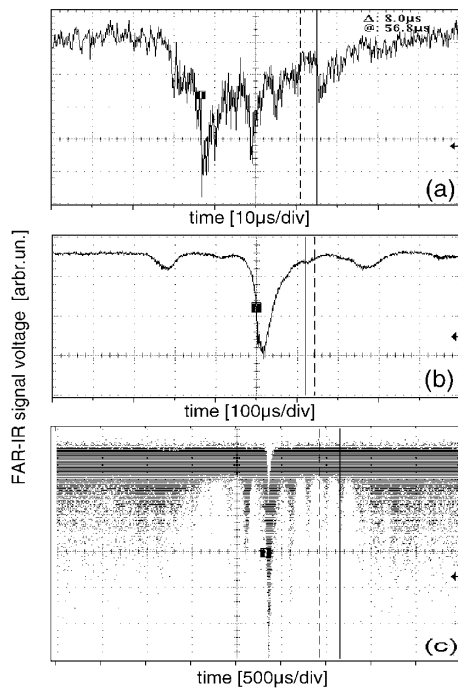


FIG. 4. Three records of larger bursts in the time domain, (a) direct, $I = 10$ mA, (b) averaged, $I = 14$ mA, and (c) persistent mode, $I = 12.5$ mA.

As seen, there is a variety of different signal amplitudes being mostly of small or even zero amplitude, typical for the bursting mode. The zero amplitude line is located on the top of the figure, including some background noise.

Similar records for the low alpha optics are shown in Fig. 3b. These signals are accumulated for 1 s. In contrast to the previous results none of the signals shows zero amplitude. To check the origin of the signal line spread, the FIR radiation was blocked by a 1 cm thick paper book, yielding the same width as before (not shown). This line width was not further broadened by the superimposed FIR signals as anticipated for constant amplitude signals. The measured behavior exemplifies the stable, steady-state character of the radiation.

Figure 4a is recorded in time domain, showing extremely fast bursting intensity pattern, fluctuating from turn to turn ($0.8 \mu\text{s}/\text{turn}$). The typical time scale is of a few μ -seconds, much shorter than the synchrotron damping time of 8 ms and the bunch rotation time $1/f_{s0}$. We expect these changes from small, sub-bunch shape modifications, leading to the fluctuating FIR intensity due to its sensitivity to the form factor f_λ .

Figure 4b displays time averaged, larger bursts, with amplitudes stronger than a given trigger level. There are few, weaker bursts adjacent to the large bursts. These lines are separated by multiples of the bunch rotation time, subharmonics of f_{s0} . The bursting bunch pattern seems to be built up over a few rotation times before the main burst and lasts a few rotation times longer, with each alternate line enhanced.

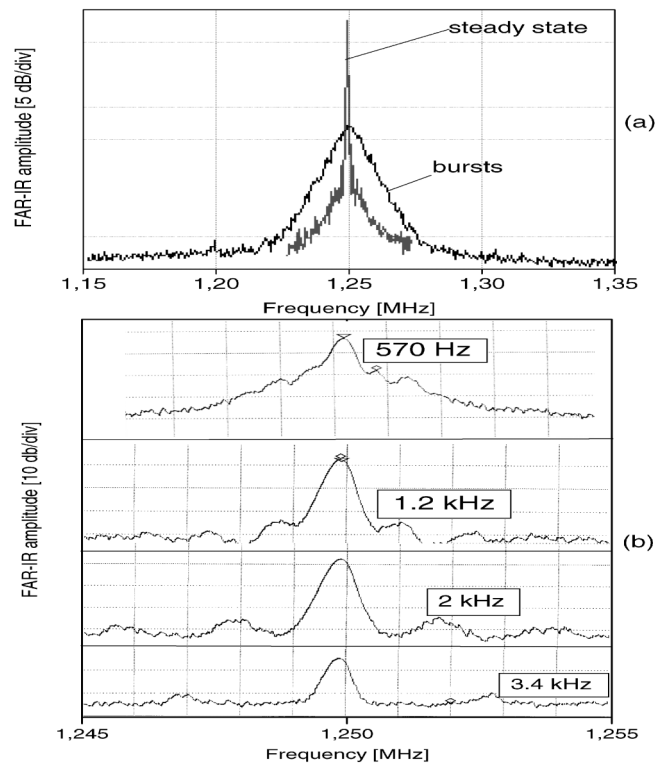


FIG. 5. FIR signals in the frequency domain, (a) bursting, $I = 14.6$ mA (for comparison, the sharp line is taken from a steady-state mode) and (b) steady-state mode at $f_s = 0.57$ kHz at $I = 6$ mA and $f_s = 1.2, 2.0,$ and 3.4 kHz at $I = 18$ mA.

Burst data on a longer time scale and acquired in a persistent record mode are shown in Fig. 4c. There is a narrow window of ± 1 ms of strongly correlated, smaller bursts around the center burst, separated by multiples of the bunch rotation time.

Figure 5a shows measurements in the frequency domain. Records of bursts with the spectrum analyzer show a broad line of about 10 kHz FWHM, centered at 1.25 MHz. Because of the stochastic time dependency a sharp line is not expected. For comparison, data of the steady-state FIR signals are included, adjusted to the same frequency scale to demonstrate the different line width.

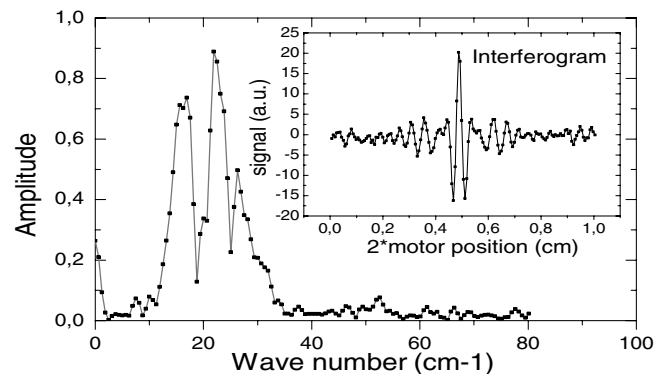


FIG. 6. Michelson interferogram and its Fourier transform, recorded at $f_s = 1.5$ kHz and $I = 12$ mA.

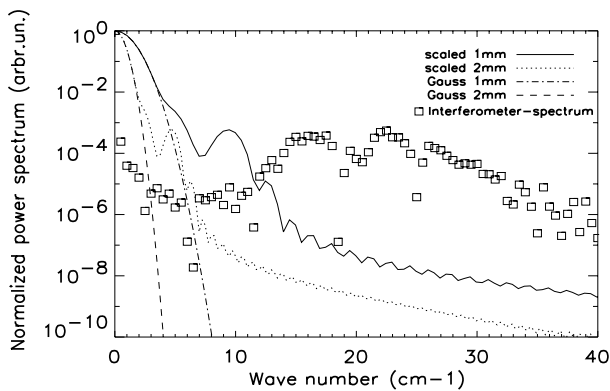


FIG. 7. Spectrum of Fig. 6 compared with the spectrum of scaled bunch shapes from streak camera measurements [6].

Figure 5b shows frequency analyzed records for the steady-state mode taken at different low α settings. A sharp line of 0.3 kHz FWHM (given by the resolution of the spectrums analyzer) and some satellite lines adjacent to the 1.25 MHz signal are seen. The first pair, shifted by the actual synchrotron frequency f_s , arises from the dipole mode of the synchrotron oscillations. The next pair, shifted by $2f_s$, originates from the quadrupole mode. There are only a few data of signal intensities as a function of different α values at fixed current. As already seen in [8], they confirm an exponential relation between signal strength and α value (not shown here). For $f_s > 3.5$ kHz ($|\alpha| > 1.6 \times 10^{-4}$) the signal vanishes below the background level. The incoherent contribution could not be detected. Absolute signal intensities are not estimated, but the strongest signal record was about a factor of 3000 above the background level. The general character of the spectrum analyzer records of the steady-state signals over the whole frequency range is not changed.

The emitted radiation was frequency analyzed by a Michelson interferometer [7]. The beam splitter of the interferometer was $12.5 \mu\text{m}$ thick, yielding a transmission rate of 1%. For a multibunch beam current of 12 mA and a tuning parameter of $f_s = 1.5$ kHz ($\alpha = +3 \times 10^{-5}$) the interferogram and its Fourier transform are shown in Fig. 6. The detected radiation is of broadband character, with intensities visible at least from 10 cm^{-1} wave numbers to 30 cm^{-1} (1 to 0.3 mm wavelength). The transmission of longer wavelengths is limited by the interferometer, shorter wavelengths are suppressed by the bunch form factor and less detector efficiency. A

strongly modulated spectrum is seen, resulting from absorption by water vapor in air.

A streak camera record of a typical bunch shape with rms length of 1.5 mm [6] was scaled to 1 and 2 mm rms length for comparison and Fourier transformed to estimate the power spectrum. As seen in Fig. 7, the calculated power spectrum shows non-Gaussian character and develops tails, ranging far into the measured frequency spectrum, much further than Gaussian bunches.

We are very grateful to P. Kuske and D. Ponwitz and our colleagues from BESSY II and DLR for valuable suggestions and technical support. Work supported by the Bundesministerium für Bildung, Wissenschaft, Forschung und Technologie and by the Land Berlin.

-
- [1] T.M. Nakazato *et al.*, Phys. Rev. Lett. **63**, 1245 (1989); E. B. Blum, U. Happek, and A.J. Sievers, Nucl. Instrum. Methods Phys. Res., Sect. A **307**, 568 (1991).
 - [2] J.S. Nodvick and D.S. Saxon, Phys. Rev. **96**, 180 (1954); R.L. Warnock and P. Morton, Part. Accel. **25**, 113 (1990); J.B. Murphy, S. Krinsky, and R.L. Gluckstern, Part. Accel. **57**, 9 (1997); S.A. Kheifets and B. Zotter, in Ref. [8], pp. 256–262.
 - [3] BESSY II Collaboration, D. Krämer *et al.*, in *Proceedings of the 7th European Particle Accelerator Conference, Vienna, 2000* (Austrian Academy of Sciences Press, Vienna, 2000).
 - [4] (a) At SURF II (NIST, Gaithersburg, MD): A.R. Hight-Walker, U. Arp, G.T. Fraser, and T.B. Lucatorto, Proc. SPIE Int. Soc. Opt. Eng. **3153**, 42 (1997); (b) at NSLS (BNL, N.Y.): G.L. Carr *et al.*, Nucl. Instrum. Methods Phys. Res., Sect. A **463**, 387–392 (2001); at MAX-I (MAX-Lab, Lund, Sweden): A. Andersson, M.S. Johnson, and B. Nelander, Opt. Eng. **39**, 3099 (2000); (d) at ALS (LBL, Berkely): J. Byrd (private communication).
 - [5] D. Robin, H. Hama, and A. Nadjj, in Ref. [9], pp. 150–164; H. Wiedemann, *Particle Accelerator Physics II* (Springer-Verlag, Berlin, 1999), Chap. 6.3.
 - [6] P. Kuske, BESSY (private communication).
 - [7] H.-W. Hübers, DLR (private communication).
 - [8] M. Abo-Bakr *et al.*, in *Proceedings of the 7th European Particle Accelerator Conference, Vienna, 2000* (Austrian Academy of Sciences Press, Vienna, 2000), p. 720.
 - [9] *Micro Bunches Workshop*, edited by E.B. Blum, M. Dienes, and J.B. Murphy, AIP Conf. Proc. 367 (AIP, New York, 1995).